Event-triggered encirclement control of multi-agent systems with bearing rigidity

Yangguang YU[1], Zhiwen ZENG[1], Zhongkui LI[2], Xiangke WANG[1]* & Lincheng SHEN[1]

[1]College of Mechatronics & Automation, National University of Defense Technology, Changsha 410073, China;
[2]State Key Laboratory for Turbulence and Complex Systems, Department of Mechanics and Aerospace Engineering, College of Engineering, Peking University, Beijing 100871, China

Abstract In recent years, the problem of multi-agent encirclement has attained much attention and was extensively studied. However, few work consider the factor that the on-board calculation as well as the communication capacity in the multi-agent system is limited. We investigate the encirclement control by employing the newly developed bearing rigidity theory and event-triggered mechanism. Firstly, in order to reduce the onboard loads, the event-triggered mechanism is considered in the framework and further an event-triggered control law based on bearing rigidity is proposed. The input-to-state stability (ISS) of networked agents is also analyzed by using the Lyapunov method and the cyclic-small-gain theory. In addition, the lower bound for the inter-event times is provided. Finally, to verify the efficiency and feasibility of the proposed encirclement control law, numerical experiments are investigated.

Keywords encirclement control, event-triggered, multi-agent system, bearing rigidity

1 Introduction

Inspired by the encircling technique that bottlenose dolphins use to entrap fishes [1] and the mysterious deadth-vortex phenomenon of ants [2], the encirclement control of networked multiple agents has attracted considerable attentions recently [3]. Similar to the so called containment problem where a collection of autonomous mobile agents are to be driven to a given target location [4, 5], the agents' motions in encirclement problem should also satisfy certain geometric constraints (usually circle). But to encircle the stationary or moving targets, the networked agents are driven to move around the centre of targets and to form a capturing formation pattern. This interesting coordination control approach can be widely applied in many areas such as coverage, patrolling, escorting and entrapment [6].

The study of the encirclement control initially stems from N-bugs problem [7]. Marshall et al. [2] proposed a formation control under cyclic pursuit for multiple agents with motion constraints in a plane. Then, the distributed cyclic pursuit approach for target capture tasks is proposed by using local distance and bearing information [8]. The underlying communication topology in these researches is assumed to

---

* Corresponding author (email: xkwang@nudt.edu.cn)

be fixed. However, owing to a variety of limitations, such as external disturbances, the topology may vary with time going by, which may cause a breakdown of system. To tackle the case of switching topology, Wen et al. [9] investigated the consensus tracking of nonlinear multi-agent systems with switching directed topology by using M-matrix approach. As bearing measurements are often cheaper and more accessible than position measurements, the bearing-only circular formation scheme was discussed in [10, 11]. To go further, Zhao et al. [12] investigated the bearing rigidity framework. In [13], Zhao et al. also addressed the problem of bearing-based network localization with a special matrix termed the Bearing Laplacian, which will be frequently used in this paper.

In many existing control methods for the multi-agent systems, a high control and communication frequency among agents is usually required in order to pursue a high control accuracy. However, in many real applications, the calculation and communication capacities of the onboard processors are quite limited, which bring many difficulties in satisfying the requirement for control and communication with high frequency. In addition, the system will run normally as long as the control accuracy reaches a specified level. A higher control accuracy may be meaningless comparing with the increased cost on the system hardware. Therefore, there should be a tradeoff between the accuracy and frequency. One way to fix this problem may be the event-trigger mechanism, as investigated in this paper. Therefore, in order to reduce on-board loads of calculation and communication, the event-triggered control method is considered in the framework of distributed multi-agent coordinations. The agents need to exchange information and update control output periodically when using traditional time-triggered control method. However, when using event-triggered control, an agent exchanges information and updates its state and output only when the specified conditions are satisfied.

In the past few years, researchers did a great deal of work in this area and many types of event-triggered control approaches are proposed, such as the continuous-time approach [14], the discrete-time approach [15] and the self-triggered approach [16]. Ref. [17] presented both centralized and decentralized form of event-triggered control for multi-agent system to solve several control problems. In a large scale and high-dimension multi-agent system, distributed control methods are often used to replace the traditional centralized control method and some other references therein [18, 19].

The event-triggered mechanism has been applied to problems such as formation control [20], filtering [21] and trajectory tracking [22]. In [23], Tallapragada proposed an event-based control algorithm for trajectory tracking in nonlinear systems. However, up to now few work combined the event-triggered mechanism with encirclement control. As the control output will stay unchanged until a certain "event" is triggered, the system may lose part of control performance. To reduce system's requirement on calculation and communication ability as much as possible and keep the control accuracy at the same time, a novel event must be defined and the trigger condition for the event should be carefully designed.

In order to reduce on-board loads, we investigate the event-triggered encirclement control problem with bearing information and the event-triggered mechanism. The first contribution of this paper is that the event-triggered mechanism is introduced into the encirclement problem. The event-triggered encirclement control law based on bearing measurements is proposed. The recently developed cyclic-small-gain theorem [24–26] as well as the bearing rigidity theory is then employed to guarantee the input-to-state stability (ISS) [27] of the closed-loop multi-agent system. In addition, we also provide the lower-bound of the inter-event times. At last, we verify the effectiveness of the event-triggered mechanism in saving computation and communication resources by numerical simulation.

This paper is organized as follows: the encirclement control problem is formulated in Section 2, where the graph theory and the bearing rigidity theory are reviewed. Section 3 proposes the event-triggered encirclement control law and studies the stability of the whole by using the Lyapunov method and the small gain theorem. Experiments and simulation results are presented in Section 4. Conclusion and future work are given in Section 5.

2 Backround and problem statement

Notation and terminology: In this paper, the null space and rank space are respectively represented as

Null$(\cdot)$ and rank$(\cdot)$. Let $I_d \in \mathbb{R}^{d \times d}$ represent the identity matrix and $\|\cdot\|$ represent the Euclidian norm of a vector or the spectral norm of a matrix. We define the operator $\otimes$ as the Kronecker product. Let $(\cdot)^{\mathrm{T}}$ denote the transposition of $(\cdot)$ and diag$(\cdot)$ be the block diagonal matrix of which the diagonal blocks are matrix $(\cdot)$. The symbols n and m are constants. $\mathbf{1}_n$ denotes a n-dimension column vector whose elements are all 1, i.e., $\mathbf{1}_n \triangleq [1, \ldots, 1]^{\mathrm{T}}$.

2.1   Bearing rigidity theory

For an undirected graph $\mathcal{G} = (\mathcal{V}, \mathcal{E})$, the vertex set is denoted as $\mathcal{V} = \{v_1, \ldots, v_n\}$ and the edge set is denoted as $\mathcal{E} \subseteq \mathcal{V} \times \mathcal{V}$ with $m = |\mathcal{E}|$. The Cartesian coordination of vertex v_i in graph $\mathcal{G}$ is denoted as $p_i \in \mathbb{R}^d$, $(d \geqslant 2)$. Then vector $p = [(p_1)^{\mathrm{T}}, \ldots, (p_n)^{\mathrm{T}}]^{\mathrm{T}} \in \mathbb{R}^{nd}$ is called a configuration of undirected graph $\mathcal{G}$ in $\mathbb{R}^d$. A framework in $\mathbb{R}^d$, denoted as $\mathcal{G}(p)$, is a combination of an undirected graph $\mathcal{G} = (\mathcal{V}, \mathcal{E})$ and a configuration p. In this paper, we suppose that no vertex in graph $\mathcal{G}$ overlaps. In other words, for $\forall i \neq j$, $p_i \neq p_j$. Then in a framework $\mathcal{G}(p)$, define

$$\phi_{ij} \triangleq p_j - p_i, \quad g_{ij} = \phi_{ij}/\|\phi_{ij}\|, \quad \forall (i, j) \in \mathcal{E}, \tag{1}$$

where unit vector g_{ij} represents the relative bearing of p_j to p_i. Note $\phi_{ij} = -\phi_{ji}$ and thus $g_{ij} = -g_{ji}$. For a nonzero vector $v \in \mathbb{R}^d (d \geqslant 2)$, define the operator $P : \mathbb{R}^d \to \mathbb{R}^{d \times d}$ as follows:

$$P(v) \triangleq I_d - \frac{v}{\|v\|} \frac{v^{\mathrm{T}}}{\|v\|}. \tag{2}$$

Note $P(v)$ (denoted as P_v in the following for notational simplicity) is an orthogonal projection operator. Any nonzero vector v will be projected onto its orthogonal compliment after the operation P. It can be easily verified that P_v satisfies $P_v^2 = P_v$ and $P_v^{\mathrm{T}} = P_v$. This orthogonal projection operator is often used for verifying whether two vectors are parallel. Thus, Ref. [12] has lemma as follows.

Lemma 1 ([12]).   Two nonzero vectors $v, u \in \mathbb{R}^d$ are parallel if and only if $P_v u = 0$ (or equivalently $P_u v = 0$).

An orientation of an undirected graph means the assignment of a direction to each edge. Then consider an arbitrary orientation of the graph $\mathcal{G}(p)$ and denote the edge vector and the bearing for the kth directed edge as follows:

$$\phi_k \triangleq p_j - p_i, \quad g_k = \phi_{ij}/\|\phi_{ij}\|, \quad \forall k \in \{1, \ldots, m\}. \tag{3}$$

Denote $\phi = [\phi_1^{\mathrm{T}}, \ldots, \phi_m^{\mathrm{T}}]^{\mathrm{T}}$ and $g = [g_1^{\mathrm{T}}, \ldots, g_m^{\mathrm{T}}]^{\mathrm{T}}$ in a compact form. Let incidence matrix $H \in \mathbb{R}^{m \times n}$ represent a $\{0, \pm 1\}$-matrix with rows indexed by edges and columns indexed by vertices. The element of H is defined as follows:

$$[H]_{ki} = \begin{cases} 1, & \text{if vertex } i \text{ is the head of edge } k, \\ -1, & \text{if vertex } i \text{ is the tail of edge } k, \\ 0, & \text{otherswise.} \end{cases} \tag{4}$$

Obviously, incidence matrix H can reflect the connection of the graph as its definition reveals. Then, in order to describe all the bearings in the framework, define the bearing function $F_{\mathrm{B}} : \mathbb{R}^{dn} \to \mathbb{R}^{dm}$ as follows:

$$F_{\mathrm{B}}(p) \triangleq [g_1^{\mathrm{T}}, \ldots, g_m^{\mathrm{T}}] \in \mathbb{R}^{dm}. \tag{5}$$

The bearing function describes all the bearings in the framework. A matrix $R_{\mathrm{b}}(p)$ called bearing rigidity matrix is defined as the Jacobian of the bearing function:

$$R_{\mathrm{b}}(p) \triangleq \frac{\partial F_{\mathrm{B}}(p)}{\partial p} \in \mathbb{R}^{dm \times dn}.$$

According to the proof in [12], $R_{\mathrm{b}}(p)$ can be expressed as

$$R_{\mathrm{b}}(p) = \mathrm{diag}\left(\frac{P_{g_k}}{\|\phi_k\|}\right)(H \otimes I_d). \tag{6}$$

Some useful properties of $R_{\mathrm{b}}(p)$ which have been proven in [12] are illustrated as follows.

Lemma 2 ([12]).   A framework $\mathcal{G}(p)$ in $\mathbb{R}^d$ always satisfies $\mathrm{span}\{\mathbf{1}_n \otimes I_d, p\} \subseteq \mathrm{Null}(R_{\mathrm{b}}(p))$ and $\mathrm{rank}(R_{\mathrm{b}}(p)) \leqslant dn - d - 1$.

Let $\tilde{\delta}p$ be a variation of the configuration p, i.e., a small change of p. If $R(p)\tilde{\delta}p = 0$, then $\tilde{\delta}p$ is called an infinitesimal bearing motion of $\mathcal{G}(p)$. An infinitesimal bearing motion is called trivial if it corresponds to a translation and a scaling of the entire framework. Then, the definition of infinitesimal bearing rigidity is given as follows.

Definition 1 (Infinitesimal bearing rigidity [12]).   A framework is infinitesimally bearing rigid if all the infinitesimal bearing motions are trivial.

Two useful lemmas related with infinitesimal bearing rigidity are given as follows.

Lemma 3 (Condition for infinitesimal bearing rigidity [12]).   For a framework $\mathcal{G}$ in $\mathbb{R}^d$, the following statements are equivalent:

(1) $\mathcal{G}$ is infinitesimally bearing rigid;

(2) $\mathrm{rank}(R(p)) = dn - d - 1$;

(3) $\mathrm{Null}(R(p)) = \mathrm{span}\{\mathbf{1}_n \otimes I_d, p\} = \mathrm{span}\{\mathbf{1}_n \otimes I_d, p - \mathbf{1}_n \otimes \overline{p}\}$, where $\overline{p} = (\mathbf{1}_n \otimes I_d)^{\mathrm{T}}p/n$ is the centroid of $\{p_i\}_{i \in \mathcal{V}}$.

Lemma 4 (Unique shape [12]).   An infinitesimally bearing rigid framework can be uniquely determined up to a translational and a scaling factor.

Remark 1.   Combined with Lemmas 3 and 4, a formation $\mathcal{G}(p)$ can be judged whether it is unique.

Based on the above notion, a special matrix $\mathcal{L}_{\mathrm{b}}(\mathcal{G}) \in \mathbb{R}^{dn \times dn}$ is defined as follows:

$$[\mathcal{L}_{\mathrm{b}}(\mathcal{G})]_{ij} = \begin{cases} \mathbf{0}_{d \times d}, & i \neq j, \ (i,j) \notin \mathcal{E}, \\ -P_{g_{ij}}, & (i,j) \in \mathcal{E}, \\ \sum\limits_{k \in \mathcal{N}_i} P_{g_{ik}}, & i = j, \ i \in \mathcal{V}, \end{cases} \tag{7}$$

where $\mathcal{N}_i \triangleq \{j \in \mathcal{V} | (i,j) \in \mathcal{E}\}$ represents the neighbor nodes of node i.

Note that matrix $\mathcal{L}_{\mathrm{b}}(\mathcal{G})$ has a similar form as the graph Laplacian matrix of $\mathcal{G}$. In addition, matrix $\mathcal{L}_{\mathrm{b}}(\mathcal{G})$ contains the inter-neighbor bearing information. Therefore, the matrix $\mathcal{L}_{\mathrm{b}}(\mathcal{G})$ is called Bearing Laplacian [13]. According to the definition in (7), Bearing Laplacian $\mathcal{L}_{\mathrm{b}}(\mathcal{G})$ can be represented as

$$\mathcal{L}_{\mathrm{b}}(\mathcal{G}) = (H^{\mathrm{T}} \otimes I_d)\mathrm{diag}(P_{g_{ij}})(H \otimes I_d), \tag{8}$$

where H is the matrix defined in (4).

With the property of orthogonal projection matrix $P_{g_{ij}} = P_{g_{ij}}^2$ and $P_{g_{ij}} = P_{g_{ij}}^{\mathrm{T}}$, the Bearing Laplacian $\mathcal{L}_{\mathrm{b}}(\mathcal{G})$ can be rewritten as follows:

$$\mathcal{L}_{\mathrm{b}}(\mathcal{G}) = (H^{\mathrm{T}} \otimes I_d)\mathrm{diag}(P_{g_{ij}})\mathrm{diag}(P_{g_{ij}})(H \otimes I_d) = \tilde{R}_{\mathrm{b}}(p)^{\mathrm{T}}\tilde{R}_{\mathrm{b}}(p), \tag{9}$$

where $\tilde{R}_{\mathrm{b}}(p) = \mathrm{diag}(P_{g_{ij}})(H^{\mathrm{T}} \otimes I_d)$. By comparing $\tilde{R}_{\mathrm{b}}(p)$ with the original definition of bearing rigidity matrix in (6), we can easily find $\tilde{R}_{\mathrm{b}}(p)$ is almost the same with the bearing rigidity matrix (see (6)) except the item $\|\phi_k\|$ part. Thus $\tilde{R}_{\mathrm{b}}(p)$ should have the same properties as $R_{\mathrm{b}}(p)$ in Lemma 2. For notational simplicity, $\tilde{R}_{\mathrm{b}}(p)$ will be denoted as $\tilde{R}_{\mathrm{b}}$ in the rests of the paper if there is no confusion.

Finally, some useful properties of Bearing Laplacian $\mathcal{L}_{\mathrm{b}}(\mathcal{G})$ are given in the following lemma.

Lemma 5 ([13]).   For an undirected graph $\mathcal{G}$, its Bearing Laplacian matrix $\mathcal{L}_{\mathrm{b}}(\mathcal{G})$ has properties as follows:

(1) $\mathcal{L}_{\mathrm{b}}(\mathcal{G})$ is positive semi-definite and symmetrical;

(2) $\mathrm{rank}(\mathcal{L}_{\mathrm{b}}(\mathcal{G})) \leqslant dn - d - 1$ and $\mathrm{Null}(\mathcal{L}_{\mathrm{b}}(\mathcal{G})) \supseteq \mathrm{span}\{\mathbf{1}_n \otimes I_d, p\}$;

(3) $\mathrm{rank}(\mathcal{L}_{\mathrm{b}}(\mathcal{G})) = dn - d - 1$ and $\mathrm{Null}(\mathcal{L}_{\mathrm{b}}(\mathcal{G})) = \mathrm{span}\{\mathbf{1}_n \otimes I_d, p\}$ if and only if $\mathcal{G}(p)$ is infinitesimal bearing rigidity.

2.2 Problem formulation

Considering a system composing of n agents, if the communication among agents is bidirectional, then its topology structure can be represented by an undirected graph $\mathcal{G}$. Each agent is represented by a node in $\mathcal{G}$ while each communication link between two agents is represented by an edge.

Suppose every agent's motion follows a single integrator model,

$$\dot{p}_i = \mu_i, \quad i = 1, 2, \ldots, n, \tag{10}$$

where $p_i \in \mathbb{R}^d$ and $\mu_i \in \mathbb{R}^d$ represent the position and control input of agent i, respectively. Let $p = [p_1^{\mathrm{T}}, \ldots, p_n^{\mathrm{T}}]^{\mathrm{T}} \in \mathbb{R}^{nd}$ and $\mu = [\mu_1^{\mathrm{T}}, \ldots, \mu_n^{\mathrm{T}}]^{\mathrm{T}} \in \mathbb{R}^{nd}$ represent the vectors of agents' positions and control inputs, respectively. After assigning an arbitrary direction for each edge in the graph, the edge vectors and bearing vectors can be denoted as $\phi = [\phi_1^{\mathrm{T}}, \ldots, \phi_m^{\mathrm{T}}]^{\mathrm{T}}$ and $g = [g_1^{\mathrm{T}}, \ldots, g_m^{\mathrm{T}}]^{\mathrm{T}}$. An agent pair $(i, j) \in \mathcal{E}$ if and only if the relative bearing information of agent i to agent j, namely g_{ij}, can be sensed by agent i. Thus, at time t, the set of relative bearing information of agent i to its neighbor agents can be denoted as $g_{ij}(t)_{j \in \mathcal{N}_i}$. Consider a moving target T, its position and velocity are represented as p_T and $\dot{p}_T$. If target T can be detected by agent i, the relative bearing of agent i to target T is represented as $g_{iT} = (p_T - p_i)/\|p_T - p_i\|$. Let p_i^* and p_j^* be the ideal positions for agent i and agent j. Then, the bearing constraints g_{ij}^* and g_{iT}^* are defined as follows:

$$g_{ij}^* = (p_j^* - p_i^*)/\|p_j^* - p_i^*\|, \tag{11}$$

$$g_{iT}^* = (p_T - p_i^*)/\|p_T - p_i^*\|. \tag{12}$$

Define the center and scale of the multi-agent system as

$$c(t) \triangleq \frac{1}{n} \sum_{i=1}^{n} p_i = \frac{1}{n}(\mathbf{1}_n \otimes I_d)^{\mathrm{T}} p, \tag{13}$$

$$s(t) \triangleq \sqrt{\frac{1}{n} \sum_{i=1}^{n} \|p_i - c(t)\|^2} = \frac{1}{\sqrt{n}} \|p - \mathbf{1}_n \otimes c(t)\|, \tag{14}$$

$c(t)$ and $s(t)$ represent the center and scale of the multi-agent system, respectively.

In order to associate the multi-agent system with the undirected graph, a sensible assumption is given as follows.

Assumption 1. all agents cannot acquire their global positions directly, but only can access into the relative bearing and relative position with respect to their neighbors and targets as well as the velocity of the target.

Thus, based on graph $\mathcal{G}$, we obtain the augmented graph $\hat{\mathcal{G}}$ consisting of n agents and target T as illustrated in Figure 1. The corresponding node set of augmented graph $\hat{\mathcal{G}}$ is $\hat{\mathcal{V}} = \{v_1, \ldots, v_n, v_{n+1}\}$ while the edge set is $\hat{\mathcal{E}} = \{e_1, \ldots, e_m, e_{m+1}, \ldots, e_{m+n}\}$.

To achieve encirclement, the agents are supposed to satisfied the following conditions:

$$\lim_{t \to \infty} \|p_i - p_t\| = \overline{r}(t) \to 0, \quad i = 1, \ldots, n,$$

$$\lim_{t \to \infty} v_1(t)/\overline{r}(t) = \cdots = \lim_{t \to \infty} v_n(t)/\overline{r}(t),$$

$$\lim_{t \to \infty} w_1(t) = \cdots = \lim_{t \to \infty} w_n(t) = \overline{w},$$

$$\lim_{t \to \infty} \psi_1(t) = \cdots = \lim_{t \to \infty} \psi_n(t) = \overline{\psi},$$

in which, $\overline{r}(t)$ is the time-varying radius of the encirclement circle; $\overline{w}$ is the angular speed of encircling; $\overline{\psi}$ is the expected angle between neighbors. Honestly, the control target described above is not intuitive; and it is very difficult to design the control law. However, while the formation of multi-agent system rotates around the geometric center, it forms an encirclement behavior. Then, we can transform this problem into the target formation problem with time-varying bearing constraints.
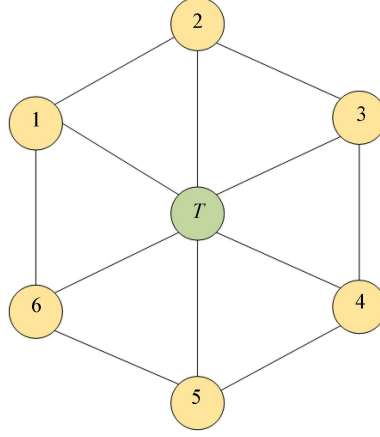
Figure 1 (Color online) Augmented graph $\hat{\mathcal{G}}$ with 6 agents and tartget T.

Definition 2 (Target formation). If $\mathcal{G}(p(t))$ is the graph of target formation, then it should satisfy following constraints:

(1) bearing constraint. $g_{ij}//g_{ij}^*$, $g_{iT}//g_{iT}^*$, $\forall (i,j) \in \mathcal{E}$;

(2) formation center constraint. $\lim_{t \to \infty} c(t) \to p_T(t)$;

(3) formation scale constraint. $\lim_{t \to \infty} s(t) \to 0$;

where binary operator $//$ represents that two nonzero vectors are parallel. $g_{ij}^*(t)$ and $g_{iT}^*(t)$ are time-varying bearing constraints defined in (11) and (12), and the geometry configuration determined by $g_{ij}^*(t)$ is a predefined regular polygon.

As listed above, the geometry configuration of formation determined by the bearing constraints should be a regular polygon. In essence, the key problem to achieve encirclement through target formation is how to make that condition guaranteed. According to the definition of bearing rigidity in Definition 1, the augmented graph $\hat{\mathcal{G}}$ is infinitesimally bearing rigid. When the bearing constraints of every pair of neighbor nodes are given, the geometry configuration is determined (the shape is unique but the scale varies). Thus, we firstly assign n agents on the unit circle evenly, and then calculate $g_{ij}^*(0)$ and $g_{iT}^*(0)$, which are the initial bearing constraints defined in (11) and (12), respectively. A regular hexagon determined by bearing constraints is illustrated in Figure 2. It is easy to verify that the geometry configuration constrained by $\{g_{ij}^*(0)\}_{j \in \mathcal{N}_i} \bigcup \{g_{iT}^*(0)\}_{i \in \mathcal{V}}$ is infinitesimal bearing rigidity. Thus, according to Lemma 4, the framework can be uniquely determined up to a translational and a scaling factor, namely the target's position and the formation's scale.

When agents circle around a fixed point, the relationship between their current positions and initial positions can be represented by

$$p(t) = R(\theta)p(0), \tag{15}$$

where matrix $R(\theta)$ is called rotation matrix and θ is the angle that agents rotate by. Specifically, in a two-dimensional space, the rotation matrix $R(\theta)$ can be defined as follows:

$$R(\theta) = \begin{bmatrix} \cos(\theta) & -\sin(\theta) \\ \sin(\theta) & \cos(\theta) \end{bmatrix}. \tag{16}$$

As Eq. (1) indicates, the bearing constraint at time t can be represented by agents's position p. Therefore, $R(\theta)$ can also be utilized to describe the bearing constraint $g_{ij}^*(t)$, where $\theta = \overline{w}t$ and $\overline{w}$ is the given angular velocity of formation. If $\overline{w} > 0$, the formation rotates anticlockwise. Otherwise, the formation rotates clockwise. Affected by the rotation matrix, the formation's bearing constraint is time-varying. The bearing constraint at time t is given by

$$g_{ij}^*(t) = R(\theta)g_{ij}^*(0), \tag{17}$$

$$g_{iT}^*(t) = R(\theta)g_{iT}^*(0), \tag{18}$$
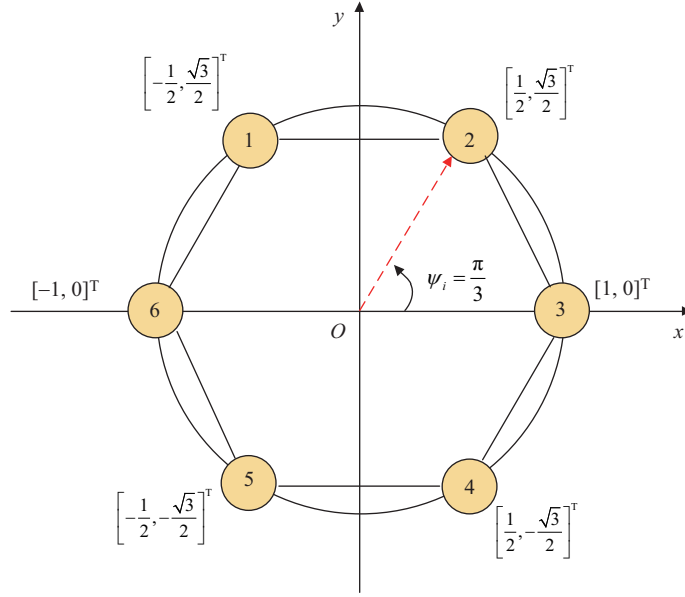
Figure 2 (Color online) A regular polygon determined by bearing constraints.

where $g_{ij}^*(0)$ and $g_{iT}^*(0)$ are initial bearing constraints at time 0.

Then, in order to reduce the on-board loads of calculation and communication, event-triggered mechanism is introduced into the system. The system communicates and updates its output only when the event-triggered condition is satisfied.

Up to this point, the problem formulation of encirclement control using bearing rigidity theory and event-triggered mechanism is completed. In the next section, control law will be provided and the stability of system will be proven.

3 Control law design and stability analysis

3.1 Control law design

To solve the proceeding encirclement control problem, a continuous control law for each agent i ($i = 1, \ldots, n$) is given as follows:

$$\mu_i(t) = -k_\alpha \sum_{j \in N_i} P_{ij}^*(t)(p_i - p_j) - k_\beta P_{iT}^*(t)(p_i - p_T) + \dot{p}_T, \tag{19}$$

where $k_\alpha > 0$ and $k_\beta > 0$ are control gain constants, and $P_{ij}^*(t)$ and $P_{iT}^*(t)$ are orthogonal projection matrices defined in (2). Specifically

$$P_{ij}^*(t) = I_d - g_{ij}^*(t)(g_{ij}^*(t))^{\mathrm{T}}, \tag{20}$$

$$P_{iT}^*(t) = I_d - g_{iT}^*(t)(g_{iT}^*(t))^{\mathrm{T}}. \tag{21}$$

As bearing constraints $g_{ij}^*(t)$ and $g_{iT}^*(t)$ are time-varying, $P_{ij}^*(t)$ and $P_{iT}^*(t)$ vary with time as well. Note that $R(\theta)R(\theta)^{\mathrm{T}} = I_d$, thus we have

$$P_{ij}^*(t) = R(\theta)P_{ij}^*(0)R(\theta)^{\mathrm{T}},$$

$$P_{iT}^*(t) = R(\theta)P_{iT}^*(0)R(\theta)^{\mathrm{T}}.$$

Based on (10) and (19), the multi-agent system can be described in a compact form as follows:

$$\dot{p}(t) = \mu(t), \tag{22}$$

$$\mu(t) = -k_\alpha \mathcal{L}_b(\mathcal{G})p - k_\beta \mathcal{D}_b(\mathcal{G})(p - \mathbf{1}_n \otimes p_T) + \mathbf{1}_n \otimes \dot{p}_T. \tag{23}$$

Block diagonal matrix $\mathcal{D}_b(\mathcal{G})$ is defined as follows:

$$\begin{cases} [\mathcal{D}_b(\mathcal{G})]_{ij} = 0, & i \neq j; \\ [\mathcal{D}_b(\mathcal{G})]_{ij} = P^*_{iT}, & i = j. \end{cases} \tag{24}$$

Further, event-triggered mechanism is considered in order to reduce the on-board loads of calculation and communication. First of all, for integrating the event-triggered mechanism, we need to define a (state) measurement error $e_i(t)$. Unlike most literatures that propose to base (state) measurement error on position information, our (state) measurement error is based on bearing information. Thus, we define a bearing state as follows:

$$x = k_\alpha \mathcal{L}_b(\mathcal{G})p + k_\beta \mathcal{D}_b(\mathcal{G})(p - \mathbf{1}_n \otimes p_T). \tag{25}$$

Obviously, x is a weighted sum of the inter-agent bearing state and the agent-target bearing state. The weighting factors imply the importance of two types of bearing state in the event-trigged mechanism. To be consistent with the control law, these two weighting factors are just set as k_α and k_β. Then, the (state) measurement error $e_i(t)$ for agent i is defined as follows:

$$e_i(t) = x_i(t) - x_i(t_k), \quad k = 1, 2, \ldots, \tag{26}$$

where t_k denotes the time when event k is triggered. Also, let $e(t) = [e_1(t), \ldots, e_n(t)]^T$ be the vector of system's state error. Thus, we have

$$e(t) = x(t) - x(t_k), \quad t \in [t_k, t_{k+1}). \tag{27}$$

Then the event trigged condition is determined by an event-triggered condition $f(e(t), x(t)) = 0$. Each time when the event-triggered condition is satisfied, every agent will communicate with other agents and further update its control input μ_i. Between two events, the control intput μ remains constant until next event is triggered, i.e., $\mu(t) = \mu(t_k)$ for all $t \in [t_k, t_{k+1})$. Therefore, combined with (23) and (25), we have the following event-triggered control law:

$$\mu(t) = -x(t_k) + \mathbf{1}_n \otimes \dot{p}_T, \quad \forall t \in [t_k, t_{k+1}). \tag{28}$$

Further, combined with (27), we rewrite control law (28) as follows:

$$\mu(t) = -x(t) + e(t) + \mathbf{1}_n \otimes \dot{p}_T. \tag{29}$$

Up to this point, we have designed the control law of encirclement for multi-agent system based on event-triggered mechanism. In the following section, we will show that the system is stable and will be convergent to the expected state under control law (29).

3.2 Stability analysis

In order to prove the stability of the multi-agent system, the structure of system is firstly explored. According to the definiton of target formation in Definition 2, the bearing constraints $g_{ij}//g^*_{ij}$ and $g_{iT}//g^*_{iT}$ should be satisfied during the process of encirclement. Further, according to Lemma 1, the condition $P^*_{ij}g_{ij} = 0$ should always hold if bearing vectors g_{ij} and g^*_{ij} are parallel, where P^*_{ij} is the orthogonal projection matrix defined in (20). Similarly, the condition $P^*_{iT}g_{iT} = 0$ should always hold if $g_{iT}//g^*_{iT}$.
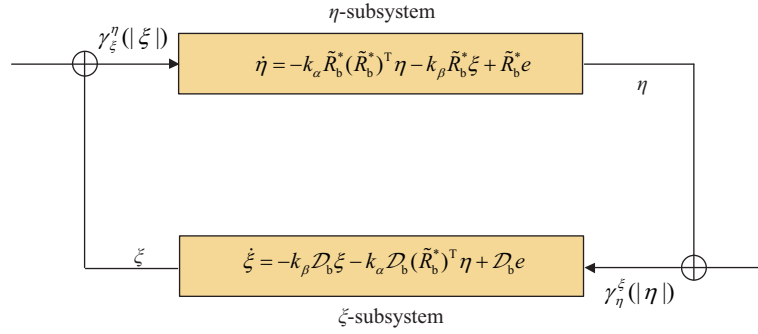
Define a variable η as follows:

$$\eta = \tilde{R}^*_b p,$$

where $\tilde{R}^*_b = \text{diag}(P^*_{ij})(H^T \otimes I_d)$. Note that $\phi = (H^T \otimes I_d)p$, thus η can be rewritten as

$$\begin{aligned} \eta &= \text{diag}(P^*_{ij})(H^T \otimes I_d)p \\ &= \text{diag}(\|\phi_l\| P^*_l) \left[\frac{\phi_1}{\|\phi_1\|}, \ldots, \frac{\phi_m}{\|\phi_m\|} \right] \\ &= \text{diag}(\|\phi_l\|)[P^*_1 g_1, \ldots, P^*_m g_m]^T, \end{aligned}$$

Figure 3 (Color online) The combination-loop control system consisting of η-subsystem and ξ-subsystem.

where $l = 1, 2, \ldots, m$ is the order number of the graph edge corresponding to agent pair (i, j).

Obviously, $\eta = 0$ if and only if $P_l^* g_l = 0$, which is the condition for $g_l // g_l^*$. Therefore, condition $g_{ij} // g_{ij}^*$ will be satisfied if $\eta = 0$. Likewise, define a varible ξ as follows:

$$\xi = \mathcal{D}_{\mathrm{b}}(p - \mathbf{1}_n \otimes p_T),$$

where $\mathcal{D}_{\mathrm{b}}$ is the target-bearing diagonal matrix defined in (24). When $p_i \neq p_T$ and $\xi = 0$, condition $g_{iT} // g_{iT}^*$ is satisfied. Therefore, we can check whether conditions $g_{ij} // g_{ij}^*$ and $g_{iT} // g_{iT}^*$ are satisfied by analysing the property of η and ξ.

Firstly, differentiating η with (9), (22), (25) and (29), we obtain the η-subsystem as follows:

$$\dot{\eta} = -k_\alpha \tilde{R}_{\mathrm{b}}^* \tilde{R}_{\mathrm{b}}^{\mathrm{T}} \eta - k_\beta \tilde{R}_{\mathrm{b}}^* \xi + \tilde{R}_{\mathrm{b}}^* (\mathbf{1}_n \otimes \dot{p}_T) + \tilde{R}_{\mathrm{b}}^* e. \tag{30}$$

From Lemma 2, we obtain that for a framework $\mathcal{G}(p)$ in $\mathbb{R}^d$, $\mathrm{span}\{\mathbf{1}_n \otimes I_d, p\} \subset \mathrm{Null}(R_{\mathrm{b}}^*)$ always holds. Therefore, $\tilde{R}_{\mathrm{b}}^* (\mathbf{1}_n \otimes \dot{p}_T) = 0$ and further the η-subsystem becomes

$$\dot{\eta} = -k_\alpha \tilde{R}_{\mathrm{b}}^* (\tilde{R}_{\mathrm{b}}^*)^{\mathrm{T}} \eta - k_\beta \tilde{R}_{\mathrm{b}}^* \xi + \tilde{R}_{\mathrm{b}}^* e. \tag{31}$$

In analogy to the η-subsystem, we differentiate ξ and obtain the ξ-subsystem as follows:

$$\begin{aligned}
\dot{\xi} &= -\mathcal{D}_{\mathrm{b}}(k_\alpha \mathcal{L}_{\mathrm{b}} p + k_\beta \xi - e) \\
&= -k_\beta \mathcal{D}_{\mathrm{b}} \xi - k_\alpha \mathcal{D}_{\mathrm{b}}(\tilde{R}_{\mathrm{b}}^*)^{\mathrm{T}} \eta + \mathcal{D}_{\mathrm{b}} e.
\end{aligned} \tag{32}$$

From (31) and (32), it can be observed that the combination-loop control system consisting of η-subsystem and ξ-subsystem is a typical interacting feedback system, as illustrated in Figure 3. In order to prove the stability of the η-subsystem and the ξ-subsystem, we first define the Lyapunov function (see [24]) of the η-subsystem and the ξ-subsystem respectively as follows:

$$V_\eta = \frac{1}{2} \eta^{\mathrm{T}} \eta, \tag{33}$$

$$V_\xi = \frac{1}{2} \xi^{\mathrm{T}} \xi. \tag{34}$$

Then, we give two lemmas related with the stability of the η-subsystem and the ξ-subsystem.

Lemma 6. For multi-agent system $\dot{p} = \mu$ with control law (29), if the trigger condition of system satisfies

$$\|e\| \leqslant \frac{\sigma_1 \|\eta\|}{\|\tilde{R}_{\mathrm{b}}^*\|}, \tag{35}$$

then the η-subsystem with ξ being the system input is input-to-state stable (ISS). Also, for any $s \in \mathbb{R}^+$, the ISS Lyapunov function defined in (33) satisfies

$$V_\eta \geqslant \gamma_\xi^\eta(V_\xi) \Rightarrow \nabla V_\eta \dot{\eta} \leqslant -2\varepsilon V_\eta, \tag{36}$$

where constants σ_1 and ε satisfy $0 < \sigma_1 < k_\alpha \lambda_2(\mathcal{L}_b)$, $0 < \varepsilon < k_\alpha \lambda_2(\mathcal{L}_b) - \sigma_1$, and the gain is given as

$$\gamma_\xi^\eta(s) = \left(\frac{k_\beta \|\tilde{R}_b^*\|}{k_\alpha \lambda_2(\mathcal{L}_b) - \sigma_1 - \varepsilon} \right)^2 s.$$

Proof. Combining with (31), we obtain the derivative of V_η as follows:

$$\dot{V}_\eta = -k_\alpha \eta^{\mathrm{T}} \tilde{R}_b^* (\tilde{R}_b^*)^{\mathrm{T}} \eta - k_\beta \eta^{\mathrm{T}} \tilde{R}_b^* \xi + \eta^{\mathrm{T}} \tilde{R}_b^* e.$$

For a positive semi-definite matrix A, let $\lambda_2(A)$ denote its smallest eigenvalue and $\mathrm{Null}(A)^\perp$ denote the orthogonal complement space of $\mathrm{Null}(A)$. Then for any vector $v \in \mathrm{Null}(A)^\perp$, it should always satisfy (see [26])

$$v^{\mathrm{T}} A v \geqslant \lambda_2(A) v^{\mathrm{T}} v. \tag{37}$$

Note that $\tilde{R}_b^* (\tilde{R}_b^*)^{\mathrm{T}} = \mathcal{L}_b^{\mathrm{T}}$ is positive semi-definite. It can be deduced from the definition $\eta = \tilde{R}_b^* p$ that η belongs to the range space of $\tilde{R}_b^*$, namely the complement space of $\mathrm{Null}(\tilde{R}_b^*)$. Therefore, $\eta \subset \mathrm{Null}(\tilde{R}_b^*)^\perp$. According to (37) and event-triggered condition (35), we have

$$\begin{aligned}\dot{V}_\eta \leqslant & -k_\alpha \lambda_2(\mathcal{L}_b)\|\eta\|^2 + k_\beta \|\tilde{R}_b^*\|\|\xi\|\|\eta\| + \|\tilde{R}_b^*\|\|\eta\|\|e\| \\ \leqslant & -\|\eta\|(k_\alpha \lambda_2(\mathcal{L}_b)\|\eta\| - k_\beta \|\tilde{R}_b^*\|\|\xi\| - \sigma_1\|\eta\|).\end{aligned} \tag{38}$$

For any given constant $0 < \varepsilon < k_\alpha. \lambda_2(\mathcal{L}_b) - \sigma_1$, it can be deduced from the given gain condition $V_\eta \geqslant \gamma_\xi^\eta(V_\xi)$ that

$$\|\xi\| \leqslant \frac{k_\alpha \lambda_2(\mathcal{L}_b) - \sigma_1 - \varepsilon}{k_\beta \|\tilde{R}_b^*\|} \|\eta\|. \tag{39}$$

Substitute (39) into (38), we get $\nabla V_\eta \dot{\eta} \leqslant -2\varepsilon V_\eta$ and the proof is complete.

Lemma 7. For multi-agent system $\dot{p} = \mu$ with control law (29), if the trigger condition of system satisfies

$$\|e\| \leqslant \frac{\sigma_2 \|\xi\|}{\|\mathcal{D}_b\|}, \tag{40}$$

then the η-subsystem with ξ being the system input is ISS. Also, for any $s \in \mathbb{R}^+$, the ISS Lyapunov function defined in (34) satisfies

$$V_\xi \geqslant \gamma_\eta^\xi(V_\eta) \Rightarrow \nabla V_\xi \dot{\xi} \leqslant -2\zeta V_\xi, \tag{41}$$

where constants σ_2 and ζ satisfy $0 < \sigma_2 < k_\beta \lambda_2(\mathcal{D}_b)$, $0 < \zeta < k_\beta \lambda_2(\mathcal{D}_b) - \sigma_2$, and the gain is given as

$$\gamma_\eta^\xi(s) = \left(\frac{k_\alpha \|\mathcal{D}_b \tilde{R}_b^*\|}{k_\beta \lambda_2(\mathcal{D}_b) - \sigma_2 - \zeta} \right)^2 s.$$

Proof. Note that $\mathcal{D}_b$ is positive semi-definite and $\xi \subset \mathrm{Null}(\mathcal{D}_b)^\perp$ as $\xi = \mathcal{D}_b(p - \mathbf{1}_n \otimes p_t)$. According to (37) and event-triggered condition (40), we have

$$\begin{aligned}\dot{V}_\xi = & -\xi^{\mathrm{T}}(k_\beta \mathcal{D}_b \xi + k_\alpha \mathcal{D}_b (\tilde{R}_b^*)^{\mathrm{T}} \eta - \mathcal{D}_b e) \\ \leqslant & -\|\xi\|(k_\beta \lambda_2(\mathcal{D}_b)\|\xi\| - k_\alpha \|\mathcal{D}_b \tilde{R}_b^*\|\|\eta\| - \|\mathcal{D}_b\|\|e\|) \\ \leqslant & -\|\xi\|(k_\beta \lambda_2(\mathcal{D}_b)\|\xi\| - k_\alpha \|\mathcal{D}_b \tilde{R}_b^*\|\|\eta\| - \sigma_2\|\xi\|).\end{aligned} \tag{42}$$

For any given constant $0 < \sigma_2 < k_\beta \lambda_2(\mathcal{D}_b)$ and $0 < \zeta < k_\beta \lambda_2(\mathcal{D}_b) - \sigma_2$, we have

$$\|\eta\| \leqslant \frac{k_\beta \lambda_2(\mathcal{D}_b) - \sigma_2 - \zeta}{k_\alpha \|\mathcal{D}_b \tilde{R}_b^*\|} \|\xi\|. \tag{43}$$

Finally, we get $\nabla V_\xi \dot{\xi} \leqslant -2\zeta V_\xi$ by substituting (43) into (42). The proof is complete.

Then, we are ready to prove the stability of system and the main result of this paper is given as follows.

Theorem 1. For multi-agent system $\dot{p} = \mu$, the control law (29) and event-triggered conditions (35) and (40) will make the system achieve the encirclement of a moving target, that is, constraints $g_{ij}//g_{ij}^{*}$, $g_{iT}//g_{iT}^{*}$, $\lim_{t\to\infty} c(t) \to p_T(t)$ and $\lim_{t\to\infty} s(t) \to 0$ will be satisfied. In addition, the formation scale $s(t)$ will shrink at a exponential-like rate and the shrink rate is estimated as follows:

$$s(t) \leqslant e^{-\frac{k_{\alpha}}{\sqrt{n}}\lambda_2(\mathcal{L}_{b})t} s(0), \quad t \geqslant 0. \tag{44}$$

Proof. In Theorem 1, three types of constraints defined in Definition 2 should be satisfied with the given control law and event-triggered condition. Therefore, in order to prove Theorem 1, we need to explore whether these constraints are satisfied.

Firstly, from Lemmas 6 and 7, we obtain that both η-subsystem and ξ-subsystem are ISS. Let Id stand for the identity function: $\text{Id}(r) = r$ for all r. Then, according to the small gain theory (see [28]), the interconnected system consisting of the η-subsystem and the ξ-subsystem is ISS when the gain of the feedback interconnected subsystem satisfies $\gamma_{\xi}^{\eta} \circ \gamma_{\eta}^{\xi} <$ Id. An ISS system with zero input must be a global asymptotic stable system. Therefore, the interconnected system consisting of the η-subsystem and the ξ-subsystem is global asymptotic stable. Further $g_{ij}//g_{ij}^{*}$ and $g_{it}//g_{it}^{*}$ hold as well.

Next, it should be proven that the multi-agent formation can track the target and $\lim_{t\to\infty} c(t) \to p_t$. Define the variable δ for the error between formation's center and target's position as follows:

$$\delta = c - p_t. \tag{45}$$

Differentiate both sides of (45) and we have

$$\begin{aligned}
\dot{\delta} &= \frac{1}{n}(\mathbf{1}_n \otimes I_d)^{\mathrm{T}}\dot{p} - \dot{p}_T \\
&= -\frac{1}{n}(\mathbf{1}_n \otimes I_d)^{\mathrm{T}}(k_{\alpha}\mathcal{L}_{b}p + k_{\beta}\mathcal{D}_{b}(p - \mathbf{1}_n \otimes p_T) - e).
\end{aligned} \tag{46}$$

According to Lemma 5, $\text{Null}(\mathcal{L}_{b}(\mathcal{G})) \supseteq \text{span}\{\mathbf{1}_n \otimes I_d, p\}$. Thus $k_{\alpha}(\mathbf{1}_n \otimes I_d)^{\mathrm{T}}\mathcal{L}_{b}p = 0$ as $\mathcal{L}_{b}(\mathbf{1}_n \otimes I_d) = 0$. Therefore, Eq. (46) can be simplified as

$$\dot{\delta} = -\frac{1}{n}(\mathbf{1}_n \otimes I_d)^{\mathrm{T}}(k_{\beta}\xi - e). \tag{47}$$

Eq. (47) reveals that the δ-subsystem is a linear system with only inputs ξ and e. Therefore, the δ-subsystem is also ISS. From what discussed above, we obtain the conclusion that the ξ-subsystem is global asymptotic stable. Following, based on the event-trigged condition $\|e\| \leqslant \sigma_2\|\xi\|/\|\mathcal{D}_{b}\|$, we have $e \to 0$ if $\xi \to 0$. Further, e-subsystem is global asymptotic stable. Therefore, the δ-subsystem is also global asymptotic stable and $\lim_{t\to\infty} c(t) \to p_T$.

Next, the formation scale should be proven to be convergent to zero with control law (29). For analysis convenience, an orthogonal projection matrix $Q_{\mathrm{M}} \in \mathbb{R}^{nd \times nd}$ is defined as follows:

$$Q_{\mathrm{M}} = \begin{bmatrix} \frac{1}{n} & \cdots & \frac{1}{n} \\ \vdots & \ddots & \vdots \\ \frac{1}{n} & \cdots & \frac{1}{n} \end{bmatrix} \otimes I_d. \tag{48}$$

This projection matrix will project a vector into the subspace $\text{span}\{\mathbf{1}_n \otimes I_d\}$. In analogy to Q_{M}, define another orthogonal projection matrix $Q_{\mathrm{M}}^{\perp}$ as follows:

$$Q_{\mathrm{M}}^{\perp} = I_n \otimes I_d - Q_{\mathrm{M}} = \begin{bmatrix} 1 - \frac{1}{n} & \cdots & -\frac{1}{n} \\ \vdots & \ddots & \vdots \\ -\frac{1}{n} & \cdots & 1 - \frac{1}{n} \end{bmatrix} \otimes I_d. \tag{49}$$

Similar to Q_{M}, $Q_{\mathrm{M}}^{\perp}$ will project a vector into $\text{span}\{\mathbf{1}_n \otimes I_d\}$'s orthogonal complement space $\text{span}\{\mathbf{1}_n \otimes I_d\}^{\perp}$.

According to the definition of orthogonal projection matrix, it can be easily verified that $Q_{\mathrm{M}} = Q_{\mathrm{M}}^2$, $Q_{\mathrm{M}}^\perp = (Q_{\mathrm{M}}^\perp)^2$ and $Q_{\mathrm{M}} Q_{\mathrm{M}}^\perp = Q_{\mathrm{M}}^\perp Q_{\mathrm{M}} = \mathbf{0}$.

Then, according to the definition of formation's center $c(t) = (1/n)(\mathbf{1}_n \otimes I_d)^{\mathrm{T}} p$, we have

$$p - \mathbf{1}_n \otimes c(t) = p - Q_{\mathrm{M}} p = Q_{\mathrm{M}}^\perp p. \tag{50}$$

Thus, the formation scale defined in (14) can be rewritten as

$$s(t) = \frac{1}{\sqrt{n}} \| Q_{\mathrm{M}}^\perp p \|. \tag{51}$$

Choose Lyapunov function V_s as follows:

$$V_s = s(t).$$

Using the property that $Q_{\mathrm{M}}^\perp Q_{\mathrm{M}} = 0$, we get the derivative of $s(t)$ as follows:

$$\dot{s}(t) = -\frac{1}{\sqrt{n}} \frac{(Q_{\mathrm{M}}^\perp p)^{\mathrm{T}}}{\| Q_{\mathrm{M}}^\perp p \|} (I_n \otimes I_d - Q_{\mathrm{M}}) \dot{p}$$
$$= \frac{1}{\sqrt{n}} \frac{(Q_{\mathrm{M}}^\perp p)^{\mathrm{T}}}{\| Q_{\mathrm{M}}^\perp p \|} \dot{p}. \tag{52}$$

According to Lemma 5, the subspace $\mathrm{span}\{\mathbf{1}_n \otimes I_d, p\}$ is a subset of Bearing Laplacian $\mathcal{L}_{\mathrm{b}}$'s kernel space. Thus we have

$$\mathcal{L}_{\mathrm{b}}(\mathbf{1}_n \otimes c(t)) = 0. \tag{53}$$

Likewise, according to the definition of $Q_{\mathrm{M}}^\perp$, $Q_{\mathrm{M}}^\perp p$ belongs to the subspace $\mathrm{span}\{\mathbf{1}_n \otimes I_d\}$'s kernel space. Therefore, it holds that

$$(Q_{\mathrm{M}}^\perp p)^{\mathrm{T}} \dot{p}_T = 0. \tag{54}$$

Then comebining with (50), (53) and (54), Eq. (52) becomes

$$\dot{s}(t) = -\frac{k_\alpha}{\sqrt{n}} \frac{(Q_{\mathrm{M}}^\perp p)^{\mathrm{T}}}{\| Q_{\mathrm{M}}^\perp p \|} \mathcal{L}_{\mathrm{b}}(p - \mathbf{1}_n \otimes c(t) + \mathbf{1}_n \otimes c(t)) - \frac{1}{\sqrt{n}} \frac{(Q_{\mathrm{M}}^\perp p)^{\mathrm{T}}}{\| Q_{\mathrm{M}}^\perp p \|} e$$
$$\qquad - \frac{k_\beta}{\sqrt{n}} \frac{(Q_{\mathrm{M}}^\perp p)^{\mathrm{T}}}{\| Q_{\mathrm{M}}^\perp p \|} \mathcal{D}_{\mathrm{b}}(p - \mathbf{1}_n \otimes c(t) + \mathbf{1}_n \otimes c(t) - \mathbf{1}_n \otimes p_T)$$
$$= -\frac{k_\alpha}{\sqrt{n}} \frac{(Q_{\mathrm{M}}^\perp p)^{\mathrm{T}}}{\| Q_{\mathrm{M}}^\perp p \|} \mathcal{L}_{\mathrm{b}}(Q_{\mathrm{M}}^\perp p) - \frac{1}{\sqrt{n}} \frac{(Q_{\mathrm{M}}^\perp p)^{\mathrm{T}}}{\| Q_{\mathrm{M}}^\perp p \|} e$$
$$\qquad - \frac{k_\beta}{\sqrt{n}} \frac{(Q_{\mathrm{M}}^\perp p)^{\mathrm{T}}}{\| Q_{\mathrm{M}}^\perp p \|} \mathcal{D}_{\mathrm{b}}(Q_{\mathrm{M}}^\perp p + \mathbf{1}_n \otimes c - \mathbf{1}_n \otimes p_T)$$
$$= -\frac{k_\alpha}{\sqrt{n}} \frac{(Q_{\mathrm{M}}^\perp p)^{\mathrm{T}}}{\| Q_{\mathrm{M}}^\perp p \|} \mathcal{L}_{\mathrm{b}}(Q_{\mathrm{M}}^\perp p) - \frac{1}{\sqrt{n}} \frac{(Q_{\mathrm{M}}^\perp p)^{\mathrm{T}}}{\| Q_{\mathrm{M}}^\perp p \|} e$$
$$\qquad - \frac{k_\beta}{\sqrt{n}} \frac{(Q_{\mathrm{M}}^\perp p)^{\mathrm{T}}}{\| Q_{\mathrm{M}}^\perp p \|} \mathcal{D}_{\mathrm{b}}(Q_{\mathrm{M}}^\perp p + \mathbf{1}_n \otimes \delta). \tag{55}$$

According to the property of the orthogonal projection matrix, $Q_{\mathrm{M}}^\perp p$ is the orthogonal compliment subspace of $\mathcal{L}_{\mathrm{b}}$'s kernel space. Thus we have

$$(Q_{\mathrm{M}}^\perp p)^{\mathrm{T}} \mathcal{L}_{\mathrm{b}}(Q_{\mathrm{M}}^\perp p) \geqslant \lambda_2(\mathcal{L}_{\mathrm{b}}) \| Q_{\mathrm{M}}^\perp p \|.$$

As target-bearing diagonal matrix $\mathcal{D}_{\mathrm{b}}$ is positive semi-definite, it holds that

$$(Q_{\mathrm{M}}^\perp p)^{\mathrm{T}} \mathcal{D}_{\mathrm{b}}(Q_{\mathrm{M}}^\perp p) \geqslant 0.$$

Combined with (55), the derivative of V_s should satisfy

$$\dot{V}_s \leqslant \underbrace{-\frac{k_\alpha}{\sqrt{n}}\lambda_2(\mathcal{L}_{\mathrm{b}})s}_{\mathrm{S}_1} + \underbrace{\frac{k_\beta}{\sqrt{n}}\|\mathbf{1}_n \otimes \delta\|}_{\mathrm{S}_2} + \underbrace{\frac{1}{\sqrt{n}}\|e\|}_{\mathrm{S}_3}.$$

As discussed in the previous section, the δ-subsystem and the e-subsystem is global asymptotic stable, namely $\delta \to 0$ and $e \to 0$ as $t \to \infty$. Obviously, when $\delta \to 0$ and $e \to 0$, the shrinking rate of formation is determined by item S_1

$$\dot{V}_s \leqslant \mathrm{e}^{-\frac{k_\alpha}{\sqrt{n}}\lambda_2(\mathcal{L}_{\mathrm{b}})}s,$$

and $s(t)$ will be convergent to zero at an exponential-like rate. Thus we obtain

$$V_s(s(t)) \leqslant \mathrm{e}^{-\frac{k_\alpha}{\sqrt{n}}\lambda_2(\mathcal{L}_{\mathrm{b}})}V_s(s(0)), \quad t \geqslant 0.$$

Finally, for $V_s = s(t)$, the shrinking rate is estimated as

$$s(t) \leqslant \mathrm{e}^{-\frac{k_\alpha}{\sqrt{n}}\lambda_2(\mathcal{L}_{\mathrm{b}})}s(0), \quad t \geqslant 0.$$

In the above discussion, it has been proven that the formation can satisfy all the required constraints during the encirclement process. Thus Theorem 1 is proven and the proof is complete.

In the final part of this section, we will show that the proposed control policy attains a strictly positive lower bound on the inter-event times. We will prove that in a method similar to that used in [17]. As the control law has two event-triggered conditions, we need to find the lower bound on the inter-event times of both conditions respectively. Then the smaller one should be the lower bound on the inter-event times for the multi-agent system.

Theorem 2. For multi-agent system $\dot{p} = \mu$, the control law (29) and the event-triggered conditions (35) and (40) will make the inter-event time lower bounded by a strictly positive time τ which is given by

$$\tau = \min\left\{\frac{\sigma_1}{C_1 C_2(\|\tilde{R}_{\mathrm{b}}^*\| + \sigma_1 M)}, \frac{\sigma_2}{\tilde{C}_1 \tilde{C}_2(\|\mathcal{D}_{\mathrm{b}}\| + \sigma_2 \tilde{M})}\right\},$$

where strictly positive constants $C_1, C_2, M, \tilde{C}_1, \tilde{C}_2, \tilde{M}$ are given as follows:

$$C_1 = k_\alpha\|\tilde{R}_{\mathrm{b}}^*\| + \frac{k_\alpha\lambda_2(\mathcal{L}_{\mathrm{b}}) - \sigma_1 - \varepsilon}{\|\tilde{R}_{\mathrm{b}}^*\|},$$

$$C_2 = \|k_\alpha\mathcal{L}_{\mathrm{b}} + k_\beta\mathcal{D}_{\mathrm{b}}\|,$$

$$M = \max\left\{\frac{\|\tilde{R}_{\mathrm{b}}^*\|}{C_2}, \frac{1}{C_1}\right\},$$

$$\tilde{C}_1 = \frac{\|\tilde{R}_{\mathrm{b}}^*\|(k_\beta\lambda_2(\mathcal{D}_{\mathrm{b}}) - \sigma_2 - \zeta)}{\|\mathcal{D}_{\mathrm{b}}\tilde{R}_{\mathrm{b}}^*\|} + k_\beta,$$

$$\tilde{C}_2 = C_2,$$

$$\tilde{M} = \max\left\{\frac{\|\mathcal{D}_{\mathrm{b}}^*\|}{\tilde{C}_2}, \frac{1}{\tilde{C}_1}\right\}.$$

Proof. Firstly, we will prove that event-triggered condition (35) has a posive lower bound on the inter-event times. As mentioned before, subspace $\mathrm{span}\{\mathbf{1}_n \otimes I_d, p\}$ is a subset of the Bearing Laplacian $\mathcal{L}_{\mathrm{b}}$'s kernel space. Thus we have $R_{\mathrm{b}}^*(\mathbf{1}_n \otimes \dot{p}_T) = 0$ and further $R_{\mathrm{b}}^*\dot{p} = -R_{\mathrm{b}}^*x + R_{\mathrm{b}}^*e$, where x is the bearing state defined in (25). It also can be verified that $\dot{x} = -(k_\alpha\mathcal{L}_{\mathrm{b}} + k_\beta\mathcal{D}_{\mathrm{b}})x$. Then we compute the time derivative of $\|e\|/\|\eta\|$:

$$\frac{\mathrm{d}}{\mathrm{d}t}\frac{\|e\|}{\|\eta\|} = \frac{e^{\mathrm{T}}\dot{e}}{\|e\|\|\eta\|} - \frac{\|e\|\eta^{\mathrm{T}}\dot{\eta}}{\|\eta\|^3}$$

$$
\begin{aligned}
&= -\frac{e^{\mathrm{T}}(k_\alpha \mathcal{L}_{\mathrm{b}} + k_\beta \mathcal{D}_{\mathrm{b}})x}{\|e\|\|\eta\|} - \frac{\|e\|\eta^{\mathrm{T}}\tilde{R}_{\mathrm{b}}^*(e-x)}{\|\eta\|^3} \\
&\leqslant \frac{\|k_\alpha \mathcal{L}_{\mathrm{b}} + k_\beta \mathcal{D}_{\mathrm{b}}\|\|x\|}{\|\eta\|} + \frac{\|e\|\|\tilde{R}_{\mathrm{b}}^*\|(\|e\| + \|x\|)}{\|\eta\|^2} \\
&\leqslant C_2 \frac{(\|e\| + \|x\|)}{\|\eta\|} + \frac{\|e\|\|\tilde{R}_{\mathrm{b}}^*\|(\|e\| + \|x\|)}{\|\eta\|^2} \\
&= C_2 \left(1 + \frac{\|\tilde{R}_{\mathrm{b}}^*\|\|e\|}{C_2\|\eta\|} \right) \frac{(\|e\| + \|x\|)}{\|\eta\|}.
\end{aligned}
$$

Combining with (39), we have

$$
\begin{aligned}
\|x\| &\leqslant k_\alpha \|(\tilde{R}_{\mathrm{b}}^*)^{\mathrm{T}}\|\|\tilde{R}_{\mathrm{b}}^* p\| + k_\beta \|\xi\| \\
&\leqslant \left(k_\alpha \|\tilde{R}_{\mathrm{b}}^*\| + \frac{k_\alpha \lambda_2(\mathcal{L}_{\mathrm{b}}) - \sigma_1 - \varepsilon}{\|\tilde{R}_{\mathrm{b}}^*\|} \right) \|\eta\| \\
&= C_1 \|\eta\|.
\end{aligned}
$$

Thus, we have

$$
\begin{aligned}
\frac{\mathrm{d}}{\mathrm{dt}} \frac{\|e\|}{\|\eta\|} &\leqslant C_1 C_2 \left(1 + \frac{\|\tilde{R}_{\mathrm{b}}^*\|\|e\|}{C_2\|\eta\|} \right) \left(1 + \frac{\|e\|}{C_1\|\eta\|} \right) \\
&\leqslant C_1 C_2 \left(1 + M\frac{\|e\|}{\|\eta\|} \right)^2.
\end{aligned}
$$

Using the notation $y = \frac{\|e\|}{\|\eta\|}$, we have $\dot{y} \leqslant C_1 C_2 (1 + My)^2$.

So y satisfies the bound $y(t) \leqslant \varphi(t, \varphi_0)$, where $\varphi(t, \varphi_0)$ is the solution of $\dot{\varphi} \leqslant C_1 C_2(1 + M\varphi)^2$, $\varphi(0, \varphi_0) = \varphi_0$.

Thus the solution of the above differential equation is given by

$$
\varphi(\tau_1, 0) = \frac{C_1 C_2 \tau_1}{1 - C_1 C_2 M \tau_1}, \tag{56}
$$

where constant τ_1 is the lower bound of the inter-event time for event-triggered condition (35).

On the other hand, the event-triggered condition (35) reveals that the inter-event times should be bounded by

$$
\varphi(\tau_1, 0) = \frac{\sigma_1}{\|\tilde{R}_{\mathrm{b}}^*\|}. \tag{57}
$$

Combining with (56) and (57), we obtain the inter-event times' lower bound

$$
\tau_1 = \frac{\sigma_1}{C_1 C_2(\|\tilde{R}_{\mathrm{b}}^*\| + \sigma_1 M)},
$$

obviously, constant τ_1 is strictly positive.

Next, we continue to prove that the inter-event times for condition (40) is lower bounded by a strictly positive constant by a similar method.

Firstly, it can be easily verified that $\dot{p} - \mathbf{1}_n \otimes \dot{p}_T = -x + e$. Then we compute the time derivative of $\|e\|/\|\xi\|$ as before

$$
\begin{aligned}
\frac{\mathrm{d}}{\mathrm{dt}} \frac{\|e\|}{\|\xi\|} &= \frac{e^{\mathrm{T}}\dot{e}}{\|e\|\|\xi\|} - \frac{\|e\|\xi^{\mathrm{T}}\dot{\xi}}{\|\xi\|^3} \\
&= -\frac{e^{\mathrm{T}}(k_\alpha \mathcal{L}_{\mathrm{b}} + k_\beta \mathcal{D}_{\mathrm{b}})x}{\|e\|\|\xi\|} - \frac{\|e\|\xi^{\mathrm{T}}\mathcal{D}_{\mathrm{b}}(e-x)}{\|\xi\|^3}
\end{aligned}
$$

$$\leqslant \frac{\|k_\alpha \mathcal{L}_{\mathrm{b}} + k_\beta \mathcal{D}_{\mathrm{b}}\|\|x\|}{\|\xi\|} + \frac{\|e\|\|\mathcal{D}_{\mathrm{b}}\|(\|e\| + \|x\|)}{\|\xi\|^2}$$

$$\leqslant \tilde{C}_2 \frac{(\|e\| + \|x\|)}{\|\xi\|} + \frac{\|e\|\|\mathcal{D}_{\mathrm{b}}\|(\|e\| + \|x\|)}{\|\xi\|^2}$$

$$= \tilde{C}_2 \left(1 + \frac{\|\mathcal{D}_{\mathrm{b}}\|\|e\|}{\tilde{C}_2\|\xi\|}\right) \frac{(\|e\| + \|x\|)}{\|\xi\|}.$$

Combining with (43), we have

$$\|x\| \leqslant k_\alpha \|(\tilde{R}_{\mathrm{b}}^*)^{\mathrm{T}}\|\|\tilde{R}_{\mathrm{b}}^* p\| + k_\beta \|\xi\|$$

$$\leqslant \left(\frac{\|\tilde{R}_{\mathrm{b}}^*\|(k_\beta \lambda_2(\mathcal{D}_{\mathrm{b}}) - \sigma_2 - \zeta)}{\|\mathcal{D}_{\mathrm{b}} \tilde{R}_{\mathrm{b}}^*\|} + k_\beta\right) \|\xi\|$$

$$= \tilde{C}_1 \|\xi\|.$$

Thus, we have

$$\frac{\mathrm{d}}{\mathrm{d}t} \frac{\|e\|}{\|\xi\|} \leqslant \tilde{C}_1 \tilde{C}_2 \left(1 + \frac{\|\mathcal{D}_{\mathrm{b}}\|\|e\|}{\tilde{C}_2\|\xi\|}\right)\left(1 + \frac{\|e\|}{\tilde{C}_1\|\xi\|}\right) \leqslant \tilde{C}_1 \tilde{C}_2 \left(1 + \tilde{M}\frac{\|e\|}{\|\xi\|}\right)^2.$$

Then using the same trick as proving the existence of τ_1, we can obtain the conclusion that inter-event time is lower bounded by a strictly positive time:

$$\tau_2 = \frac{\sigma_2}{\tilde{C}_1 \tilde{C}_2(\|\mathcal{D}_{\mathrm{b}}\| + \sigma_2 \tilde{M})}.$$

Through the above analysis, the inter-event times for both event-triggered conditions are lower bounded by a strictly positive constant. When either of the event-triggered condition is satisfied, the event for system will be triggered. Thus, the inter-event time for system should always be the smaller one of the two constants τ_1 and τ_2, namely $\tau = \min\{\tau_1, \tau_2\}$. The proof is complete.

4   Simulations

To verify the effectiveness of the proposed control law, we present a simulation in which six agents encircle a moving target in a two-dimensional space. The initial expected formation is illustrated in Figure 2. The initial inter-agent bearing constraints are as follows: $g_{12}^* = -g_{21}^* = [1,0]^{\mathrm{T}}$, $g_{23}^* = -g_{32}^* = [1/2, \sqrt{3}/2]^{\mathrm{T}}$, $g_{34}^* = -g_{43}^* = [-1/2, -\sqrt{3}/2]^{\mathrm{T}}$, $g_{45}^* = -g_{54}^* = [-1,0]^{\mathrm{T}}$, $g_{56}^* = -g_{65}^* = [-1/2, \sqrt{3}/2]^{\mathrm{T}}$, $g_{61}^* = -g_{16}^* = [1/2, \sqrt{3}/2]^{\mathrm{T}}$. The initial agent-target bearing constraints are as follows: $g_{1T}^* = [1/2, -\sqrt{3}/2]^{\mathrm{T}}$, $g_{2T}^* = [1/2, \sqrt{3}/2]^{\mathrm{T}}$, $g_{3T}^* = [-1,0]^{\mathrm{T}}$, $g_{4T}^* = [-1/2, \sqrt{3}/2]^{\mathrm{T}}$, $g_{5T}^* = [-1/2, -\sqrt{3}/2]^{\mathrm{T}}$, $g_{6T}^* = [1,0]^{\mathrm{T}}$. Set the initial positions of the target as $p_T = [100, 100]$ m and the velocity of the moving target as $\dot{p}_T = [1, 0.5]^{\mathrm{T}}$ m/s. The initial positions of agents are $[380, 130]^{\mathrm{T}}$ m, $[-195, 280]^{\mathrm{T}}$ m, $[215, 0]^{\mathrm{T}}$ m, $[120, -100]^{\mathrm{T}}$ m, $[80, -220]^{\mathrm{T}}$ m, $[-100, -25]^{\mathrm{T}}$ m. Set the gain coefficient of the control law (29) as $k_\alpha = 1$, $k_\beta = 0.5$ and the constants of event-triggered conditions as $\sigma_1 = \sigma_2 = 1$. The sampling time of simulation is set as 0.05 s. The rotation matrix $R(\theta)$ is defined as (16), where $\theta = \overline{w}t$ and $\overline{w} = -\pi/30$ (rad/s).

Then, with the control law (29) and the event-triggered conditions (35) and (40), the simulation result is illustrated from Figures 4–10. The trajectories of agents and targets during the process of encirclement are shown in Figure 4. The result shows that the multi-agent formation can encircle and track the moving target with obvious scale shrinking during the whole process. Figure 5 reveals that the distances between the target and different agents will be convergent and Figure 6 illustrates that agents will encircle the target uniformly. The variation of formation scale during the process of encirclement is illustrated in Figure 8 (depicted as blue line). It can be seen that the formation scale shrinks at an exponential-like rate after the regular formation is formed. Then, the error between formation's center and target's
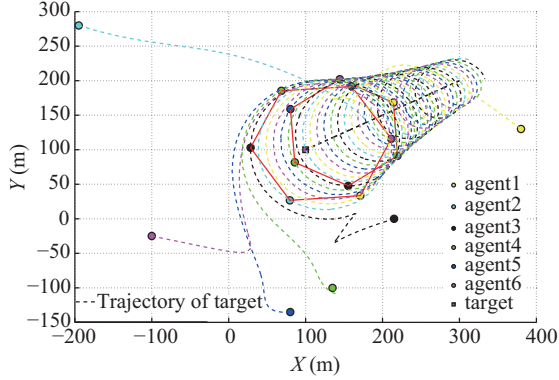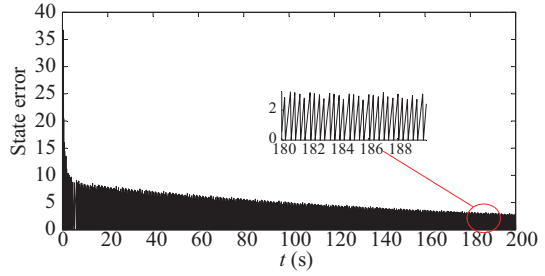
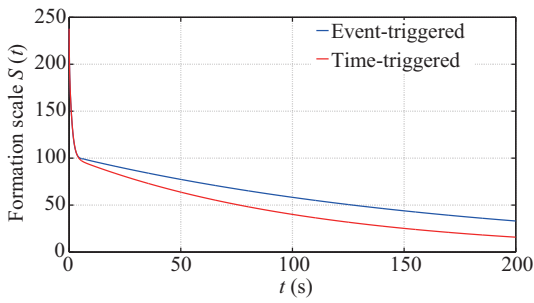**Figure 4** (Color online) Multi-agent sytem encircles a moving target.
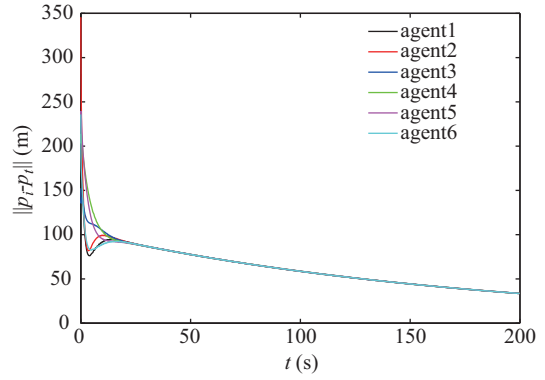
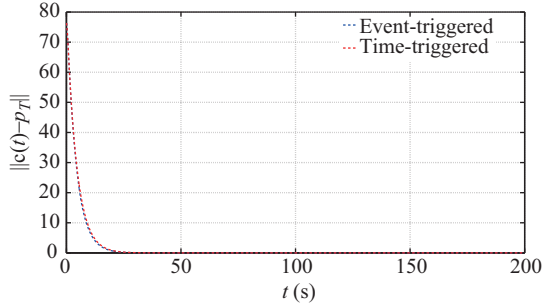**Figure 5** (Color online) The distance between agents and target.
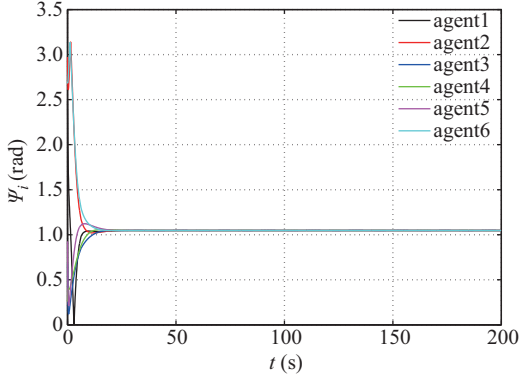
Figure 6 (Color online) The angle between neighbour agents.

Figure 7 (Color online) Evolution of state error norm.

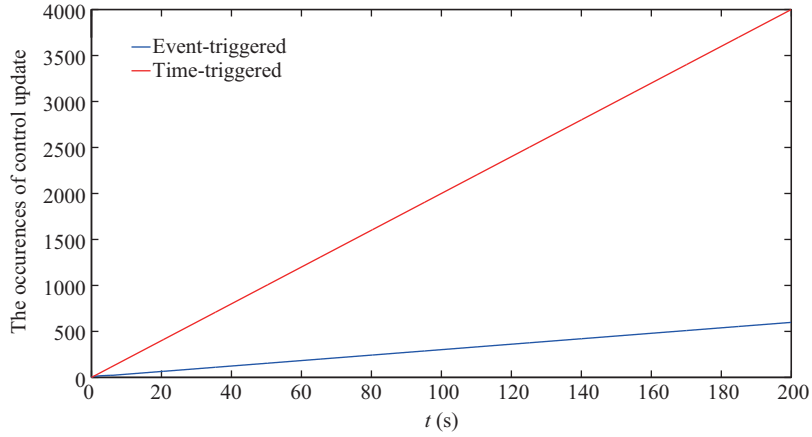**Figure 8** (Color online) The formation scale for two mechanisms.

Figure 9 (Color online) Error between formation's center and target for two mechanisms.

position is shown in Figure 9 (depicted as blue line). It can be seen that the error is convergent to zero after 30 s, which proves the system satisfies $\lim_{t\to\infty} c(t) \to p_t$. The evolution of state error is depicted in Figure 7. As shown in Figure 7, the norm of state error decreases gradually but the time between two events is always positive.

In order to find out the effects that the event-triggered mechanism brings into the system, we also simulate the situation with the time-triggered mechanism, namely using control law (23). Firstly, the errors between the formation's center and the target for two mechanisms are illustrated in Figure 9. Obviously, the difference between the event-triggered mechanism and the time-triggered mechanism is

Figure 10 (Color online) The occurrences of control update for two mechanisms.

very small. The result in Figure 9 reveals that the configuration of formation is only marginally affected by the event-triggered mechanism. Then Figure 8 illustrates the process of encirclement and the evolution of formation scale. From Figure 8, it can be found that the convergence rate of formation with the event-triggered mechanism is slightly slower than that with the time-triggered mechanism. At last, we compare the occurrences of control update for two mechanisms, which is illustrated in Figure 10. The frequency of system control update of the time-triggered is obviously higher than that of the event-triggered. In the 200-second simulation, the occurrences of control update for the time-triggered is 4000 while that for the event-triggered is only less than 600. This result means the event-triggered mechanism reduces the required control and communication frequency of the system to 15% of the previous one.

Remark 2. By comparing the simulation results of two mechanisms, it can be found that the event-triggered mechanism reduces the control and communication frequency at a small expenses of the control performance. Usually, the event-triggered mechanism could cause slightly longer convergence time and poorer control performance. However it will greatly reduce the control and communication frequency. Therefore, it is worthy of introducing the event-triggered mechanism into the system of which the calculation and communication capacity is limited.

5 Conclusion and future work

In this paper, in order to reduce the frequency of communication and control updating, we introduce the event-triggered mechanism into encirclement control. Further, based on this mechanism, we propose a bearing-based control law with aid of Bearing Laplacian matrix. Next, feasible event-triggered conditions are provided and the stability of the system is analyzed. It is proven in this paper that the system with designed control law demonstrates global asymptotic stability and will never be infinitely triggered in a finite time. Finally, numerical simulations are investigated and the performances of both event-triggered and traditional time-triggered control laws are compared in the same condition. The experiment results indicate that it is worthy of using event-triggered mechanism to reduce the computation and communication loads at a small expense of control performance.

Our work is based on the assumption that the communication and control updating of all agents happen at the same time, namely, in a centralized method. However, considering a fully decentralized system, it is hard to ensure that. In addition, a multi-agent system is often troubled by a variety of noises. Therefore, we will consider investigating the decentralized encirclement control under a noisy environment in the future. Further, we will also validate the performance of our control law with nonlinear or high-order physical robots, such as quadrotors.

Conflict of interest   The authors declare that they have no conflict of interest.

References

1 Haque M A. Biologically inspired heterogeneous multi-agent systems. Dissertation for Ph.D. Degree. Atlanta: Georgia Institute of Technology, 2010. 9–15

2 Marshall J A, Broucke M E, Francis B A. Formations of vehicles in cyclic pursuit. IEEE Trans Autom Control, 2004, 49: 1963–1974

3 Wang X, Zeng Z, Cong Y. Multi-agent distributed coordination control: developments and directions via graph viewpoint. Neurocomputing, 2016, 199: 204–218

4 Ji M, Ferrari-Trecate G, Egerstedt M, et al. Containment control in mobile networks. IEEE Trans Autom Control, 2008, 53: 1972–1975

5 Li Z, Ren W, Liu X, et al. Distributed containment control of multi-agent systems with general linear dynamics in the presence of multiple leaders. Int J Robust Nonlin Control, 2013, 23: 534–547

6 Franchi A, Petitti A, Rizzo A. Decentralized parameter estimation and observation for cooperative mobile manipulation of an unknown load using noisy measurements. In: Proceedings of the 2015 IEEE International Conference on Robotics and Automation (ICRA), Seattle, 2015. 5517–5522

7 Parrish J K, Viscido S V, Grunbaum D. Self-organized fish schools: an examination of emergent properties. Biol Bull, 2002, 202: 296–305

8 Kim T H, Sugie T. Cooperative control for target-capturing task based on a cyclic pursuit strategy. Automatica, 2007, 43: 1426–1431

9 Wen G, Duan Z, Chen G, et al. Consensus tracking of multi-agent systems with lipschitz-type node dynamics and switching topologies. IEEE Trans Circ Syst I Regul Pap, 2014, 61: 499–511

10 Zheng R, Liu Y, Sun D. Enclosing a target by nonholonomic mobile robots with bearing-only measurements. Automatica, 2015, 53: 400–407

11 Daingade S, Sinha A. Target centric cyclic pursuit using bearing angle measurements only. IFAC Proc Volume, 2014, 47: 491–496

12 Zhao S, Zelazo D. Bearing rigidity and almost global bearing-only formation stabilization. IEEE Trans Autom Control, 2016, 61: 1255–1268

13 Zhao S, Zelazo D. Localizability and distributed protocols for bearing-based network localization in arbitrary dimensions. Automatica, 2016, 69: 334–341

14 Yu H, Antsaklis P J. Event-triggered real-time scheduling for stabilization of passive and output feedback passive systems. In: Proceedings of the 2011 American Control Conference, San Francisco, 2011. 1674–1679

15 Li S, Xu B. Event-triggered control for discrete-time uncertain linear parameter-varying systems. In: Proceedings of the 32nd Chinese Control Conference, Xi'an, 2013. 273–278

16 Lemmon M, Chantem T, Hu X S, et al. On self-triggered full-information h-infinity controllers. In: Proceedings of the 10th International Conference on Hybrid Systems: Computation and Control. Berlin: Springer, 2007. 371–384

17 Dimarogonas D V, Frazzoli E, Johansson K H. Distributed event-triggered control for multi-agent systems. IEEE Trans Autom Control, 2012, 57: 1291–1297

18 Fan Y, Feng G, Wang Y, et al. Distributed event-triggered control of multi-agent systems with combinational measurements. Automatica, 2013, 49: 671–675

19 Mazo M, Tabuada P. Decentralized event-triggered control over wireless sensor/actuator networks. IEEE Trans Autom Control, 2011, 56: 2456–2461

20 Tang T, Liu Z X, Chen Z Q. Event-triggered formation control of multi-agent systems. In: Proceedings of the 30th Chinese Control Conference, Yantai, 2011. 4783–4786

21 Hu S, Yue D. Event-based h^{∞} filtering for networked system with communication delay. Signal Process, 2012, 92: 2029–2039

22 Yin X X, Yue D. Event-triggered tracking control for heterogeneous multi-agent systems with markov communication delays. J Franklin Inst, 2013, 350: 1312–1334

23 Tallapragada P, Chopra N. On event triggered tracking for nonlinear systems. IEEE Trans Autom Control, 2013, 58: 2343–2348

24 Liu T, Hill D J, Jiang Z P. Lyapunov formulation of ISS cyclic-small-gain in continuous-time dynamical networks. Automatica, 2011, 47: 2088–2093

25 Dashkovskiy S N, Rüffer B S, Wirth F R. Small gain theorems for large scale systems and construction of iss Lyapunov functions. SIAM J Control Optimiz, 2010, 48: 4089–4118

26 Wang X, Liu T, Qin J. Second-order consensus with unknown dynamics via cyclic-small-gain method. IET Control Theory Appl, 2012, 6: 2748–2756

27 Sontag E D. Smooth stabilization implies coprime factorization. IEEE Trans Autom Control, 1989, 34: 435–443

28 Jiang Z P, Mareels I M Y, Wang Y. A lyapunov formulation of the nonlinear small-gain theorem for interconnected ISS systems. Automatica, 1996, 32: 1211–1215